

FINITE DIFFERENCE APPROACH FOR RIGOROUS FULL-WAVE ANALYSIS OF SUPERCONDUCTING MICROWAVE STRUCTURES.

Mohamed A. Megahed and Samir M. El-Ghazaly

Department of Electrical Engineering, Arizona State University, Tempe, Arizona 85287-5706

Abstract:

A full-wave analysis of superconducting transmission line structures is presented. This approach avoids making any simplifying assumptions regarding the strip thickness and the electromagnetic wave inside the superconductor. The propagation constant, as well as the attenuation constant, are obtained rigorously by solving the eigen value problem resulting from the discretization of the wave equations using finite difference method. The corresponding eigen vectors are the possible modes. The current distribution inside the superconducting materials and the electromagnetic fields in the structure can be easily obtained.

1. INTRODUCTION

Strip lines and microstrip transmission lines are common waveguiding structures used in microwave and millimeter-wave systems. Many fundamental electrical parameters of the superconductor, such as the surface resistance, conductivity, critical temperature, magnetic field strength, and field penetration, can be determined by measuring the propagation characteristics and the quality factors of these devices [1]. Therefore, it is crucial to develop an accurate numerical model to determine these electrical parameters accurately from the measurements.

Previous research works have often been limited to describe the transmission line characteristic in term of its integrated quantities, and strip thickness is mostly treated by an approximation of some kind [2]-[3].

In this paper, we present a complete model which can be used for any of the transmission line structures, which include high T_c superconducting material. This model incorporates all the physical aspects, of the high T_c superconductor materials through London's equations. It also satisfies all the electromagnetically required boundary conditions in the structure using Maxwell's equations. The

physical characteristics of the superconductor are blended with the electromagnetic model by using the phenomenological two fluid model. The finite difference method is used to implement this model because it has a great deal of flexibility, and equations may be derived directly from Maxwell's equations. The complex propagation constant is calculated. The losses inside the superconductor material are evaluated. The effect of different London's penetration depth on the wave propagation characteristics is also investigated.

2. THEORETICAL ANALYSIS

The two fluid model assumes that the electron gas in a superconductor material consists of two gases, the superconducting electron gas, constituting from Cooper or electron pairs, and the normal electron gas.

$$\mathbf{J} = \mathbf{J}_n + \mathbf{J}_s \quad (1)$$

The following London's equations describe the relation between the superconductor current density and the fields [4],

$$\frac{\partial \mathbf{J}_s}{\partial t} = \frac{1}{\mu_0 \lambda^2} \mathbf{E} \quad (2)$$

$$\nabla \times \mathbf{J}_s = \frac{-1}{\lambda^2} \mathbf{H} \quad (3)$$

where λ is the penetration depth inside the superconducting material.

Maxwell's equation,

$$\nabla \times \mathbf{H} = j\omega \epsilon_0 \mathbf{E} + \mathbf{J} \quad (4)$$

when combined with eq. (1), (2) results in

$$\nabla \times \mathbf{H} = j\omega \epsilon_0 \epsilon_s \mathbf{E} \quad (5)$$

where the complex strip relative dielectric constant ϵ_s is

$$\epsilon_s = \left[\left(1 - \frac{1}{\omega^2 \mu_0 \epsilon_0 \lambda^2} \right) - j \frac{\sigma_n}{\omega \epsilon_0} \right] \quad (6)$$

Here, we assume that the electrical properties of the superconductor are isotropic. The negative dielectric constant for the superconducting strip may be explained by the stored electric kinetic energy associated with the superconductor electrons pair motion. The eigen value problem can be solved for the TM_z mode without loosing the generality of the

OF2

method. The full wave analysis can be carried out by applying the same procedure to the TE_z mode, then combining both modes together.

Assuming the waves propagate in the $+z$ direction with a propagation constant $\gamma=\alpha+\beta$, that is yet to be determined. The resulting general wave equation, in case of nonuniform dielectric constant, at each point over the structure is expressed as follows,

$$\frac{h_p^2}{\omega^2 \mu_0 \epsilon_p} \left[\frac{\partial^2 E_z}{\partial x^2} - \gamma^2 \frac{\partial}{\partial x} \left(\frac{1}{h_x^2} \frac{\partial E_z}{\partial x} \right) \right] + \frac{h_p^2}{\omega^2 \mu_0 \epsilon_p} \left[\frac{\partial^2 E_z}{\partial y^2} - \gamma^2 \frac{\partial}{\partial y} \left(\frac{1}{h_y^2} \frac{\partial E_z}{\partial y} \right) \right] + h_p^2 E_z = 0 \quad (7)$$

where $h^2 = \gamma^2 + \omega^2 \mu_0 \epsilon$, subscript x and y stands for the x and y directions, and p represents the value at any arbitrary point in the structure.

The effect of the temperature, as well as the penetration depth, on the performance of the superconductor transmission line are also addressed. The dependence of the effective penetration depth (λ) on the temperature can be expressed as follows [5],

$$\lambda(T) = \lambda(0) \left[1 - \left(\frac{T}{T_c} \right)^{1/2} \right] \quad (8)$$

where $\lambda(0)$ is the penetration depth at $T=0$, and the conductivity dependence on the temperature is stated as,

$$\sigma_n(T) = \sigma_n(T_c) \left(\frac{T}{T_c} \right)^4 \quad (9)$$

where $\sigma(T_c)$ is the conductivity at $T=T_c$.

3. NUMERICAL APPROACH

The finite difference method is used to solve the general wave equation for E_z . With the notation, as shown in Fig. 1,

$$E_{zij} = E_z(i\Delta x + j\Delta y) \quad (10)$$

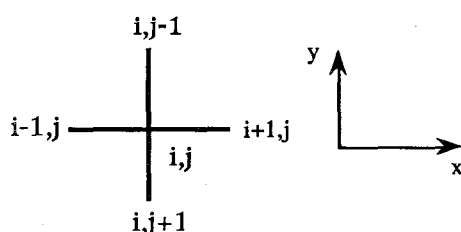


Fig. 1. ij and corresponding xy axis

Substituting in (7), and after some manipulation, we get the following general finite difference equation,

$$\begin{aligned} & \frac{1}{\Delta x^2} \left(\frac{\epsilon_{i+1,j}}{\epsilon_{ij}} \frac{h_{i,j}^2}{h_{i+1,j}^2} \right) E_{zi+1,j} + \frac{1}{\Delta x^2} \left(\frac{\epsilon_{i-1,j}}{\epsilon_{ij}} \frac{h_{i,j}^2}{h_{i-1,j}^2} \right) E_{zi-1,j} + \\ & \frac{1}{\Delta y^2} \left(\frac{\epsilon_{i,j+1}}{\epsilon_{ij}} \frac{h_{i,j}^2}{h_{i,j+1}^2} \right) E_{zi,j+1} + \frac{1}{\Delta y^2} \left(\frac{\epsilon_{i,j-1}}{\epsilon_{ij}} \frac{h_{i,j}^2}{h_{i,j-1}^2} \right) E_{zi,j-1} + \\ & \left[h_{i,j}^2 - \frac{1}{\Delta x^2} \left(\left(\frac{\epsilon_{i+1,j}}{\epsilon_{ij}} \frac{h_{i,j}^2}{h_{i+1,j}^2} \right) + \left(\frac{\epsilon_{i-1,j}}{\epsilon_{ij}} \frac{h_{i,j}^2}{h_{i-1,j}^2} \right) \right) - \right. \\ & \left. \frac{1}{\Delta y^2} \left(\left(\frac{\epsilon_{i,j+1}}{\epsilon_{ij}} \frac{h_{i,j}^2}{h_{i,j+1}^2} \right) + \left(\frac{\epsilon_{i,j-1}}{\epsilon_{ij}} \frac{h_{i,j}^2}{h_{i,j-1}^2} \right) \right) \right] E_{zi,j} = 0 \end{aligned} \quad (11)$$

where $h_{i,j}^2 = \omega^2 \mu_0 \epsilon_{ij} + \gamma^2$. The coefficients inserted are only used at the interface between the different materials constituting the structure. The discontinuities at the interface are carefully handled to satisfy the matching conditions without generating undesired numerical singularities. The discontinuity in the field in the direction perpendicular to the interface, as a result of different dielectric values at both side is treated using the electric field-dielectric constant product. This results in a finite difference scheme which is valid everywhere in the transmission line structure. There is no need to impose boundary conditions anywhere inside the structure.

Using the even symmetry of the fundamental mode, the numerical model is simulated over half of the structure. A perfect magnetic wall is inserted at the plane of symmetry. The ground plane is represented by a perfect electric plane, for simplicity. The open boundaries can be closed with perfect conducting walls, either electric or magnetic. These walls should be relatively far enough away from the strip that they do not affect the final solution.

A non-uniform mesh is generated over the transmission line cross-section. The numbers of patches are increased in the area where high fields are expected. The electric parameters are averaged over the patches lying at the interface between different materials composing the structure. The mesh is constructed such that all the interfaces and the boundaries lie exactly on one side of a patch.

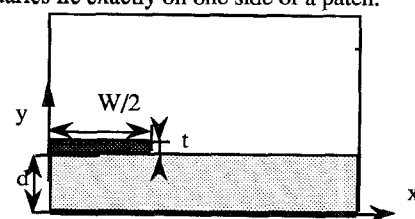


Fig. 2. Superconducting microstripe line

4. RESULTS AND DISCUSSION

Numerical results are generated for the superconductor microstripline, filled with a lossless dielectric material with $\epsilon_d = 23$, as shown in Fig. 2. The configuration has the following dimensions: strip width $W = 5000 \mu\text{m}$, substrate thickness $d = 4500 \mu\text{m}$, and superconducting strip $t = 1.0 \mu\text{m}$. The characteristics of the superconducting material are as follows, penetration depth at $T = 0 \text{ K}$ is $\lambda(0) = 0.18 \mu\text{m}$, the superconductor critical temperature, $T_c = 100 \text{ K}$, and the conductivity inside the normal electron gas at $T = T_c$ equals to $\sigma_n = 10^4 \text{ S/cm}$. The results are calculated at two different temperatures, the liquid nitrogen boiling point $T = 77 \text{ K}$, and $T = 89 \text{ K}$.

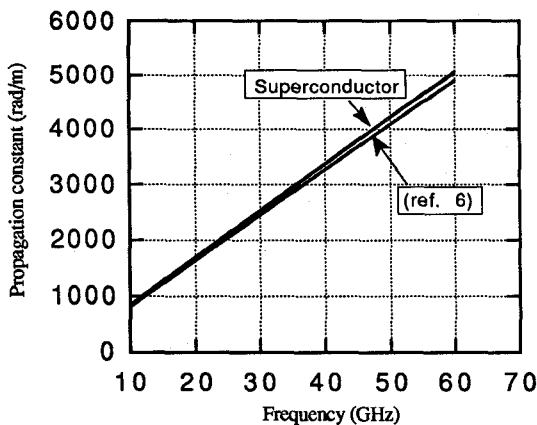


Fig. 3. Propagation constant for Microstripline filled with lossless dielectric.

The phase constant of the superconducting microstripline as function of frequency, at $T = 0 \text{ K}$, is shown in Fig. 3. The results are verified by comparing them with the phase constant of a microstripline with perfect conductors [6]. As expected, the two curves are close to each other. The phase velocity of the superconducting structure is slightly larger than that of the perfectly conducting structure due the internal inductance of the superconducting material.

The attenuation characteristics for the superconducting microstripline at different temperatures are presented in fig. 4. The attenuation increases with frequency. The attenuation also increases with temperature as expected. The corresponding phase constant and relative phase constant shift are shown in Fig. 5. The propagating mode is a TM_z mode. The effect of the superconducting material can also be observed in Fig. 5. The low dispersion of the superconducting transmission

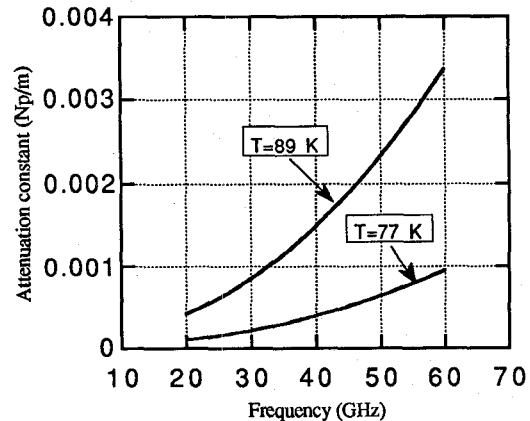


Fig. 4. Attenuation constant of Superconducting Microstripline filled with lossless dielectric.

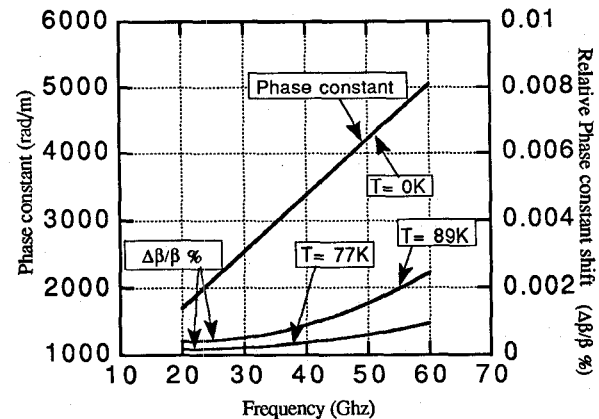


Fig. 5. Phase constant of Superconducting Microstripline filled with lossless dielectric.

line is clear. The percentage change in the phase constant at $T = 77 \text{ K}$ and $T = 89 \text{ K}$ is also depicted in Fig. 5. As the temperature increases, the phase constant slightly increases. Although, the phase constant shift is small, it is predicted by our calculations.

To study the effect of different high T_c superconductor characteristics on the line performance, structures with different London's penetration depths are investigated. All other parameters are kept the same as before. The attenuation and phase constants at $T = 77 \text{ K}$ are shown in Fig. 6 and Fig. 7, respectively. The increase in the attenuation constant with the penetration depth is due to the increase of the normal electron current penetration in the material. The increase in the phase constant can be explained by the slow wave effect

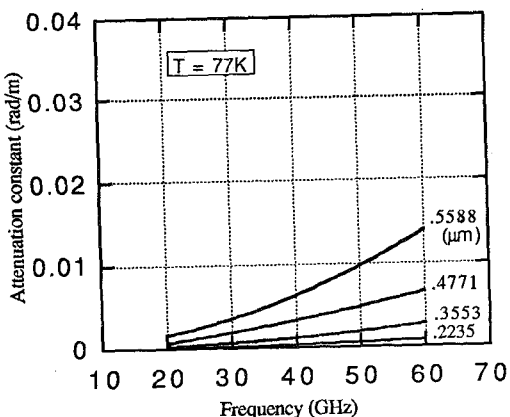


Fig. 6. Attenuation constant of Superconducting Microstripline filled with lossless dielectric at different penetration depth

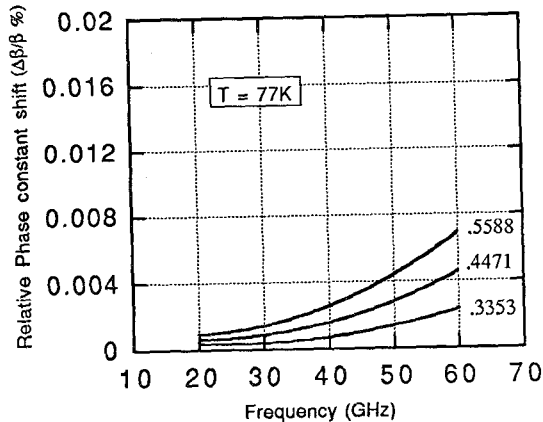


Fig. 7. Relative Phase constant of Superconducting Microstripline filled with lossless dielectric at different penetration depth

resulting from the increase in the internal inductance associated with the superconducting material. We believe that this is one of the most accurate methods to obtain the dispersion characteristics of a superconducting microwave structure.

5. CONCLUSION

A method for calculating the propagation characteristics of superconducting microwave structures, by formulating the eigen value problem that takes into account the wave propagation inside the superconductor material, is presented. This procedure is general, accurate, and yet flexible. Results for the propagation characteristics of the microstripline are demonstrated. Slow wave propagation is observed along the microstrip line. The increase of the attenuation with temperature and frequency is clearly shown.

Other characteristics of microwave superconducting lines are also presented.

References

- [1] S. M. El-Ghazaly, R. B. Hammond, and T. Itoh, "Analysis of Superconducting Microwave Structures: Application to Microstrip Lines," *IEEE Trans. Microwave Theory Tech.*, vol. 40, no. 3, pp. 499-508, 1992.
- [2] D. Nghiem, J. T. Williams, and D. R. Jackson, "A General Analysis of Propagation Along Multiple-Layer Superconducting Stripline and Microstrip Transmission Lines," *IEEE Trans. Microwave Theory Tech.*, vol. 39, no. 9, pp. 1533-1564, 1991.
- [3] J. Kessler, R. Dill, and P. Russer, "Field Theory Investigation of High-T_c Superconducting Coplanar Waveguide Transmission Lines and Resonators," *IEEE Trans. Microwave Theory Tech.*, vol. 39, no. 9, pp. 1566-1574, 1991.
- [4] F. London, *Superfluids*. New York: Wiley, vol. 1, 1950.
- [5] T. Van Duzer and C. W. Turner, *Principles of Superconductive Devices and Circuits*. New York: Elsevier, 1981.
- [6] C. A. Balanis, *Advanced Engineering Electromagnetics*. New York: Wiley, 1989.